International Journal of Innovative Computing, Information and Control
Volume **11**, Number **2**, April **2015**

ICIC International ©2015 ISSN 1349-4198
pp. 691–705

OPTIMAL LENGTH DETERMINATION OF THE MOVING AVERAGE FILTER FOR POWER SYSTEM APPLICATIONS

Abdullah I. Al-Odienat and Amneh A. Al-Mbaideen

Electrical Engineering Department
Mutah University
Mutah Street, Karak 61710, Jordan
Odienat@mutah.edu.jo

Received May 2014; revised September 2014

Abstract. *Moving average (MA) filter is widely used in power system applications as a low pass (LPF) or a high pass filter (HPF). It is used as a main processing technique or as a preprocessing step for a wide variety of signal processing applications in power system and control. The selection of the appropriate value of the MA filter length is the most significant criterion in specifying its characteristics. This work presents a novel method for identification of the MA filter length. The method is based on the independent component analysis (ICA). In power system applications, the MA filter is used for smoothing purposes or to separate the fast and slow components of the measured data. The implementation of this method is easy and straightforward. It is also adaptive with the measured data. The proposed method is validated using IEEE 30 bus model.*
Keywords: ICA, Fast varying component, Moving average filter, Power flow, Power systems

1. **Introduction.** Generally, signals are classified into time domain and frequency domain encoded signals. The NIR spectra, electromagnet interferences, and sound waves fall in the frequency domain category while the power system signals, are time domain signals. The information of the time domain signals are encoded in the shape of the signal waveform, whereas the information of the frequency domain signals are encoded in the magnitude or phase of the signal. Based on that, there are mainly two used approaches in filtering process; the frequency and time domain filtering [1]. The frequency domain filtering is obtained by converting the signal into the frequency domain using fast Fourier transform (FFT), followed by multiplying the signal by a window in the frequency domain, and finally computing the inverse FFT. The time domain filtering is performed by convolving the measured data with the filter impulse response function. The time domain filtering has the advantage over the frequency domain that the measured data can be filtered online without waiting for the whole data.

One of the most common time domain filtering is the MA filter or running filter [2-6]. MA is a finite impulse response filter (FIR) based on computing the weighted average of adjacent points. The unrivalled combination of flexibility, speed, being easy to be used and realized make MA filter one of the most popular digital filters in several disciplines. MA filter has received a great attention in chemometrics [7,8], marketing and finance [9], biomedicine [10,11], communication, and power system applications [12-16].

In the field of power systems many signal processing techniques such as neural networks, genetic algorithm, fuzzy logic, fast Fourier transform FFT, wavelet, and ICA are used. These methods allow us to effectively estimate the voltage, current, active and

reactive powers, harmonic sources, load forecasting, power quality analysis, power factor correction, power electronics, and control systems.

Several studies used the MA filter in the field of power system either as a preprocessing technique or as a main processing technique. Nakata *et al.* [12,13] introduced a technique based on moving average filter to compensate harmonic currents by using a dc filter capacitor with a high accuracy and good response. MA filter is used in harmonic identification due to their regular frequency response and sharp step response as mentioned in [14,15]. Freijedo *et al.* in [14] presents a novel algorithm for harmonic identification; it combines the moving average filtering and Fourier correlation algorithm for controlling of active filters. In [15] the MA filter is integrated with heterodyning for harmonic identification. The MA filter is used as an adaptive filter for control systems of power electronics. In [16] the filter is designed to give a step response as fast as possible while retaining good noise canceling properties.

The MA filter is combined with the neural network for short term load forecasting [17]. The results obtained in [17] show that the filter is able to handle noise, missing data and abnormal data. Forbes and his group [18] have used the MA filter to improve the dynamic response of power factor correctors (PFC). Their analysis shows that the MA filter is excellent for PFC control. In [19-31] the MA filter is used as a preprocessing step for power flow analysis based on ICA.

The MA filter requires setting only the filter length (smoothing factor) from a wide range of selectable lengths. The length of MA filter specifies the number of waveform samples that the MA will span each time. The required amount of filtering is dependent on the value of smoothing factor, type of data and the application. Increasing the smoothing factor, for instance, produces a greater smoothing and a sharp impulse response. At the same time, increasing this factor reduces the signal intensity and produces significant distortions. Therefore, the problem addressed in this study is the determination of MA filter length that provides the best smoothing process without introducing a distortion.

All the above mentioned points motivated us to introduce a new method for the determination of the appropriate value of the filter length. The proposed method preserves the adaptation between the filter length and the variation in the measured data. The proposed method combines ICA and the filtering process. Amari performance index [32,33] is used in this work as an objective function to measure filter ability to separate the fast components and select the appropriate value of the filter length. To the best of our knowledge, no method exists addressing the determination of the MA filter length.

This paper is organized as follows. Section 1 is the introduction. In Section 2 we formulated the problem addressed in this work, in Section 3 introduced the proposed technique and the basic background theory of ICA and MA filter, JADE algorithm and Amari Index. In Section 4 we presented the case study. The results and an extensive discussion for IEEE 30 bus system is presented in Section 5. In Section 6 we presented the concluded remarks of the work.

2. **Statement of the Problem.** The MA filter is a simple type of FIR filters that does not need assigning a cut-off frequency value. It is considered as one of the most common filters used for smoothing application by enhancing the long-term fluctuation and attenuating the short-term fluctuation. Compared to other linear filters with the same edge of sharpness, MA filter produces the lowest amount of noise. The possible amount of noise reduction is equal to the square-root of the number of points in the average, i.e., a 16 point filter reduces the noise by a factor of 4.

There are several types of the MA filter; the simple MA (SMA), the weighted moving average (WMA), and the exponential moving average (EMA). In this study, the SMA method is used to demonstrate the proposed algorithm.

The SMA filters can be implemented either as a one sided point or as a symmetry. The output $y(i)$ of the one sided MA filter represents the average of the present and past values each time:

$$y(i) = \frac{1}{M} \sum_{j=0}^{M-1} x(i-j) \tag{1}$$

where M is the filter length. This type of MA filter is easy to implement, however, it produces a phase shift between the output and the input. On the other hand, the symmetrical MA filter is a window of size (M) moving along the data one element each time. The middle element of the window is replaced by the weighted sum of the elements within the window, so the filtered data represents the average of the present, future, and past values each time. At the starting and the end of the data, parts of the data are usually lying outside the window, so the averaging is performed upon less data. This type of MA filter cannot be applied upon online data; it can be used for the processing of offline data only. The symmetrical MA filters are called zero phase shift filters since there is no phase shift between the input and output. The output of the symmetrical MA filter $y(i)$ can be represented by the general formula of the causal FIR filter

$$y(i) = \frac{1}{M} \sum_{j=-(M-1)/2}^{(M-1)/2} x(i-j) \tag{2}$$

where $b_k = \frac{1}{M}$.

The unit impulse response $h(n)$ of the one sided MA filter can be represented as the sum of the weighted shifted unit impulse functions

$$h[n] = \sum_{k=0}^{M} b_k \delta(n-k) \tag{3}$$

Since MA filter is a time domain filter, the output $y(n)$ and the input are related by the convolution expression

$$y[n] = \sum_{k=0}^{M} h[k]x[n-k] \tag{4}$$

The frequency response of the MA filter is the Fourier transform of the unit impulse response $h(n)$ and is given as

$$H(f) = \frac{\sin(\pi M f)}{M \sin(\pi f)} \tag{5}$$

The frequency response of the filter explains the effect of the filtering process upon each frequency. It is a complex function, so it can be represented by its amplitude and phase. The phase components describe the effect of filtering on the phase shift (delay) of each frequency component on the time domain. The amplitude component, on the other hand, represents the quantity of attenuation at each frequency component as a result of filtering.

The amplitude frequency response of the MA filter shown in Figure 1 has been computed using Equation (5). It is clear from Figure 1 that the frequency response of the filter possesses low pass characteristics. The figure shows that the MA filter has a bad performance in the frequency domain. A careful inspection of Figure 1 shows that the frequencies greater than f_s ($f_s = \frac{2\pi}{M}$) oscillates rather than going to zero and major parts

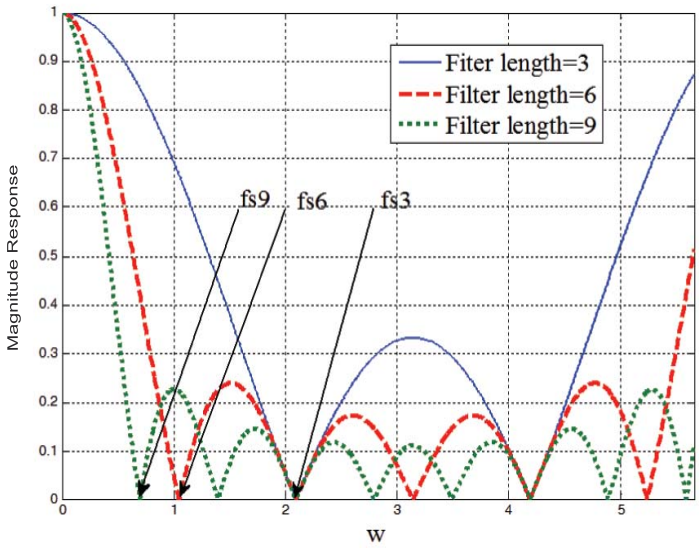

FIGURE 1. Amplitude frequency response of the MA filter for different values of the MA filter length

of the high frequency components are not removed, therefore, it possesses a weak stop-band attenuation. Additionally, the magnitude response has $M-1$ spectral zeros and is at frequencies equal to f_s or multiple of f_s.

It is also obvious from Figure 1 that increasing the filter length will sharpen the roll-off of the filter, and therefore, a large amount of the noise is filtered out. However, this will not reduce the amplitude of the side loops significantly and will increase the hidden latency on any signal passing through the filter. Latency equals to the required time for a signal to propagate through the filter (or simply it is the difference in time between the input and the response). Generally, digital filters introduce latency, which is a function of the number of delay elements in the system. Therefore, increasing the filter length will increase the number of delay elements and as a result, the latency is increased.

Passing the signals through MA filter several times can improve the stop-band attenuation of the filter. In this case the filter impulse response $h(n)$ will look like a Gaussian filter (central limit theorem). However, this reduces the sharpness of the edges of the step response of the filter in the time domain, while the filter roll-off in the frequency domain will be improved.

From the above literature review, it is clear that the most significant issue in the MA filter design is the selection of the appropriate length of the filter. Taking in consideration, that filter length is dependent on the threshold between the fast and slow fluctuation and on the field of application as well.

Therefore, there is a need for a technique to determine the appropriate value of the MA filter length. All these points motivate us to introduce a new method for the determination of the appropriate value of the filter length. The proposed method preserves the adaptation between the filter length and the variation in the measured data.

3. **MA Filter Length Estimation.** Generally, in power systems, the variation of load profiles can be characterized as a summation of two components [20,21,34]; fast varying component and slow varying component. The slow varying components, which are not statistically independent, represent hour-to-hour variations and they are due to several factors such as the weather variations. On the other hand, the fast components are a

stochastic process and they are due to the second to minute variations in the load demand. In [20], it has been shown that the fast varying components are statistically independent and have supergaussian distribution. Therefore, the load profiles of electrical system can be modeled as the sum of the fast trend (independent) and slow trend (dependent) data:

$$V = Z.I \tag{6}$$

where $I = [I_{slow} + I_{fast}]$, hence,

$$V = Z.I_{slow} + Z.I_{fast} = V_{slow} + V_{fast} \tag{7}$$

The n rows of V represent the outputs of sensors for L samples. The m rows of I are the independent components measured at L samples where I refers to the bus current. Each row in the mixing matrix Z represents the weight of each pure component in the sensor output, where Z corresponds to the network impedance. I_{slow} and I_{fast}, are the slow and fast components of the load profiles, respectively.

Several methods are used for the preprocessing of data for ICA algorithm such as PCA [35-37], filtering [38-40], and the second derivative [41-43]. Low pass filtering (LPF) is widely used to smooth signals and remove high frequency components that corrupt the observed data such as noise. The filtering operation can be achieved by using time domain filtering [37], which is obtained by multiplying the measured load profiles V by a matrix H [38], where H is a component wise filtering matrix and its elements depend on the aim of the filter; lowpass, highpass, or bandpass filter.

$$V^* = V.H = Z.I.H = Z.I^* \tag{8}$$

where V^* is the filtered data. In [44], it has been shown that the standard ICA algorithms can be used to analyze V^* since the filtering operation preserves the original mixing matrix. The extracted components I^* are the filtered form of the underline sources. The following is an example of the LPF matrix H:

$$H_{LPF} = \frac{1}{3}\begin{bmatrix} \cdots & & & \vdots & \vdots & & & \\ \cdots & 1 & 1 & 1 & 0 & 0 & 0 & \cdots \\ \cdots & 0 & 1 & 1 & 1 & 0 & 0 & \cdots \\ \cdots & 0 & 0 & 1 & 1 & 1 & 0 & \cdots \\ & & & \vdots & \vdots & & & \end{bmatrix} \tag{9}$$

The fast varying components in [20-23] have been separated from the measured data by first extracting the slow varying components $V^* = V.H = Z.I_{slow}$ using MA filter. Then the fast components are computed by subtracting the slow components from the measured data $V_{fast} = V - V^* = Z.I_{fast}$.

Figure 2 depicts the procedure of the introduced method to estimate the MA filter length. The introduced algorithm is used in this study in the analysis of power flow analysis using blind source separation [20-31]. As shown in Figure 2, the measured load profiles are used to obtain either the ac or dc power flow using Newton-Raphson method. Then apply MA filter to separate the fast components of the bus voltages as in Equation (7) for a specified filter length. The resultant fast components are then fed to ICA model to estimate the mixing matrix. In this work, the Joint Approximate Diagonalization of Eigenmatrices (JADE) algorithm [45] is used to process complex data without the need to deal with the imaginary and real parts of the data individually. The estimated mixing matrix Z is used to compute the global matrix G:

$$G = YZ \tag{10}$$

where G will be needed to compute Amari index [32,33]. The whole process is repeated for each filter length. Finally, the obtained indexes are plotted versus the filter length and the filter that gives minimum index is selected as the optimum filter length.

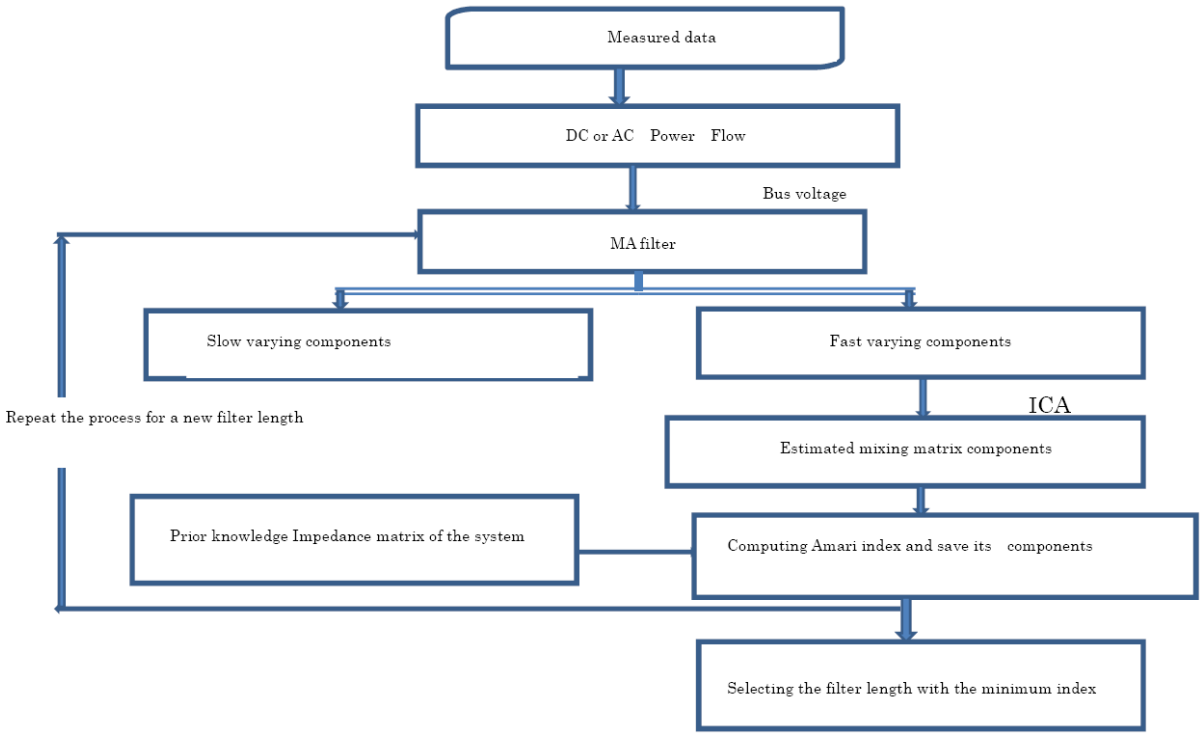

FIGURE 2. Estimation process of MA filter length

3.1. **Independent component analysis (ICA).** ICA was first introduced by Jeanny-Herault and Christian Jutten in 1986 [46]. It has attracted a great interest in different fields such as in communication, biomedical, power systems, and chemistry. ICA is a high order statistical (HOS) algorithm used for blind source separation. HOS is an extension of the first and second order measures, (such as the autocorrelation, power spectrum, and variance) to the higher orders measures (known as cumulants) [47]. The HOS measures can identify correctly the non-minimum phase signals since they are capable to preserve the phase information about the process compared to the first and second order measures [44,48]. HOS measures use the third or higher power of the sample such as the skewness and kurtosis instead of the second order measurements like the variance, first and second momentum. Moreover, HOS are less affected by the additive noise like additive white Gaussian noise since this type of noise is completely defined by the first and second order momentum.

In power systems' applications, ICA approach is used to predict the harmonic load profiles [20-30] and load forecasting [31,49]. The application of ICA approach requires that the underlying components are statistically independent, however, in the power systems, there is a degree of dependency between the basic components of the load profiles due to the slow varying components. Therefore, there is a need for a preprocessing technique to remove this dependency.

The free noise standard ICA model can be defined as

$$V = Z.I \tag{11}$$

where the n rows of V represent the outputs of sensors measured for L samples. The m rows of I are the independent components measured for L samples. Each row in the mixing matrix Z represents the weight of each pure component in the sensor output. In this paper, Z, V, and I refer to the bus current, network impedance, and bus voltage, respectively.

Regardless of the ICA method used, the main objective of the ICA algorithm is to determine the mixing matrix Z as well as the bus current I from the measured data without any prior information:

$$\hat{I} = Z^{-1}V = YV \tag{12}$$

where, $\hat{I}$ is the estimated bus current (independent components) matrix and Z^{-1} is the demixing matrix, which physically represents the admittance matrix Y. If the independent components $\hat{I}$ are extracted correctly, the product of the Z and Y is a generalized permutation matrix. There are several algorithms used to extract the independent components from the measured data such as FASTICA that based on fixed-point iteration method [50,51], (JADE) [45], Infomax ICA [52], Mean-field ICA (MF-ICA) [53], and kernel ICA (KICA) [54]. The difference between ICA methods comes from the criteria that are used to measure the independency and the optimization method.

3.2. **JADE algorithm.** JADE algorithm is developed to process off-line data. It is designed originally to deal with complex data, and this was the reason for using it in this work. Another form of this algorithm is developed to deal with the real data efficiently. Its efficient ability to estimate the mixing matrix is due to the use of the second and fourth order cumulants and matrix diagonalization technique. The algorithm requires no parameter tuning compared to other ICA algorithms. The presence of parameter tuning in ICA methods leads to different solutions for the same data depend. The data size and the number of ICs, as well as the distribution of sources influence the speed of JADE. The data size that can be used for JADE is limited and dependent on the used memory. JADE algorithm can be summarized in the following steps:

Step 1: Whitening the data matrix V

Generally, Irrespective of the used ICA algorithm the first step of the ICA is to compute the principal component model (PCA) [40-42] for the centered rows of the measured matrix. Whitening is a type of preprocessing technique aims to reduce the dimensionality of the data matrix so that most of the additive noise can be filtered. Moreover, it transforms the data matrix to have orthonormal columns. That means the covariance matrix of the whitened data equals to the identity matrix. Several methods are used for whitening such as Gram-Schmidt orthogonalisation (GSO) [55,56], PCA with their eigenvalue decomposition (EVD) and singular value decomposition (SVD) [57]. The linear whiting can be obtained by multiplying the measured matrix V by a linear matrix W:

$$W = C_x^{-1/2} = ED^{-1/2}E^T \tag{13}$$

where C_x is the covariance matrix $E[VV^T]$. The columns of E are the unit norm eigenvectors of the covariance matrix C_x. D is a diagonal matrix, the diagonal elements of which are the eigenvalues of the covariance matrix C_x. The linear matrix W is not the only unique whitening matrix.

Step 2: Cumulants Computation

In this step, JADE algorithm computes the fourth order tensor K $[n \times n \times n \times n]$, where n is the number of independent components and equals to the dimension of the rotating matrix. The diagonal of the tensor matrix is the fourth autocumulant (kurtosis) that can be defined as follows:

$$Cum_4\{V_w, V_w, V_w, V_w\} = E\{V_w\}^4 - 3.E^2\{V_w\}^2 \tag{14}$$

While the nondiagonal elements of tensor are the crosscumulant and defined as:

$$\begin{aligned}\kappa_4\{V_i, V_j, V_k, V_l\} = & E\{V_i V_j . V_k V_l\} - E\{V_i V_j\}.E\{V_k V_l\} \\ & - E\{V_i V_k\}.E\{V_j V_l\} - E\{V_i V_l\}.E\{V_j V_k\}\end{aligned} \tag{15}$$

If the vectors V_i and V_j are mutually statistically independent, the crosscumulant will be equal to zero while the autocumulant will be maximum. Based on that, JADE algorithm attempts to find the rotation matrix that diagonalizes the tensor matrix.

Step 3: Cumulants Tensor Decomposition

In this step, JADE algorithm computes the eigenvalue decomposition of the tensor matrix and produces $n(n+1)/2$ orthogonal symmetry matrix (M_i) with Frobenius norm being equal to 1. Then it projects the fourth tensor matrix into the orthogonal $n \times n$ matrices. After that, the JADE algorithm diagonalizes the eigenmatrices using Jacobi algorithm by minimizing the sum square of the off diagonal elements of the orthogonal matrices, so that M_i is transferred as follows:

$$M_i^* = M_i V \tag{16}$$

where V is the rotation matrix. Finally, the demixing matrix Y is obtained by multiplying M_i^* by the score matrix of the original data.

3.3. **Amari index.** In the present work, the performance index (PI) (known as Amari index) [26] is used to evaluate the efficiency of the MA filter and determine the appropriate length of the filter. Amari index is defined as

$$PI_i = \frac{1}{n}\sum_{j=1}^{n}\left(\frac{\sum_{i=1}^{n}|g_{ij}|}{\max_i |g_{ij}|} - 1\right) + \frac{1}{n}\sum_{i=1}^{n}\left(\frac{\sum_{j=1}^{n}|g_{ij}|}{\max_j |g_{ij}|} - 1\right) \tag{17}$$

where g_{ij} is the ijth element of Global matrix (G), which is defined as the multiplication of the mixing matrix Z and the estimated demixing matrix Y $(G = YZ)$. For perfect estimation, G should equal to the identity matrix. However, if the mixing matrix is unknown or it is not estimated perfectly for real data, the Global matrix will be a generalized permutation matrix [44,57,59], where the permutation matrix is a matrix that has only one nonzero element in each row and column. PI will be zero for statistically independent components and increase as the dependency increased.

4. **Case Study.** As it is mentioned in the introduction, the MA filter is used in several applications of power systems such as the harmonic and load forecasting analysis. In power system analysis using ICA [20-31], the MA filter is used as a low pass filter to extract the fast varying components. The ICA algorithm required that the fast components should be statistically independent in order to separate the underlying components. In all of these studies, there is no any guaranty that the fast components are statistically independent. Our proposed method is aimed at extracting the fast components so that they are statistically independent. To evaluate the performance of the proposed method, it is demonstrated on an IEEE 30-bus system [20]. The observation vector data is generated using centered and normalized typical load profiles downloaded from the website of Electric Reliability Council of Texas (ERCOT) [60]. The fast varying fluctuation is modeled by adding Laplace distribution data [61-63] with zero mean and 0.02 variance to centered and normalized load profiles. In this work, the observed vectors are varied according to 1-minute samples by manipulating the original load profiles that vary according to 15 minutes samples, so we have 1440 samples per day.

The load buses of the IEEE-30 bus model in [20] is used in this work; the loads at buses 5 and 8 are assumed constants. Bus 1 is a slack bus. The 17 load buses 2, 3, 7, 10, 14, 15,

16, 17, 18, 19, 20, 21, 23, 24, 26, 29, and 30 are generated by multiplying the active and reactive powers of each load by one of the load profiles. The observation vector for the IEEE 30 bus system is obtained by computing Newton-Raphson ac and dc power flow at each sampling test using the public domain program MATPOWER [63].

The fast and slow varying components of the observed vector are separated using MA filter of several lengths. The fast varying components are processed using JADE algorithm for complex data [64,65] to get the mixing matrix Z that will be used to estimate the independent sources, the performance index (Amari index) is then computed. This process is repeated for each MA length. The obtained performance indexes are plotted versus the filter length. The filter length that produces the minimum value of PI is selected as the optimum filter length.

5. **Discussion and Results.** The optimization method described above was applied to IEEE 30 bus. The effect of number of samples and fast components fluctuations on the optimum filter length is studied for both dc and ac power flow analysis. In each case Amari performance index is plotted versus several values of the filter length where that produced the minimum Amari index is selected as the optimum filter. Figure 3(a) is produced by adding zero mean Laplace distributed random fluctuations with 0.002 variances to the data with 1440 samples. Figure 3(a) shows that the dc power flow in the introduced method produces the best separation of the fast components as compared to ac power flow. We see in Figure 3(a) that the optimum filter length for the dc power flow is lower than that obtained for ac power flow where it is 5 and 10 for the dc and ac power flow, respectively. As compared to the ac power flow, the dc power flow has more fluctuation and at most produces high values for the Amari index.

In general, the harmonic estimation methods [20-31] require a large number of measurements that are limited because of the cost and instrumentation requirements. The performance of ICA is dependent on the number of samples since it is a statistical method. If the number of samples is less than the number of independent sources then this will lead to overlearning in ICA [66], while if the number of samples is greater than the number of sources, an artefactual (spikes and bumps) signals are produced by the ICA algorithm. On the other hand, the number of samples in digital signal processing (DSP) implies an important factor in determining the characteristics of the signal and the filter design requirements. Therefore, the impact of the sample size on the introduced method should be investigated by implementing it several times for 1440, 720, 288, and 96 samples. Amari index for each number of samples is computed and plotted versus the filter length as shown in Figures 3(a)-3(d).

Figures 3(a)-3(d) show that the proposed method has the ability to predict the optimum length of the MA filter even if the number of samples is low. The figure also shows that using dc power flow leads to clear and specified value of the filter length with the lowest value of Amari index, since the dc power flow guarantees the conditions of the ICA algorithm.

Figures 3(a)-3(d) show also that as the number of samples is decreased the optimum filter length is increased. The optimum filter length for 1440 samples is 5 and it is increased to 11, 12, 13 for number of samples 720, 288, and 96 samples respectively. The reduction in the number of samples implies that the measured signals are corrupted with more error, which required that the bandwidth of the filter should be decreased as shown in Figure 3(a). Additionally, [67] shows that even for small sample sizes, the ICA algorithm performs quite well, and it is confirmed that the estimation error decreases with an increase of the number of samples. Obviously, the curves of the ac power flow analysis have less fluctuation compared to that of the dc analysis.

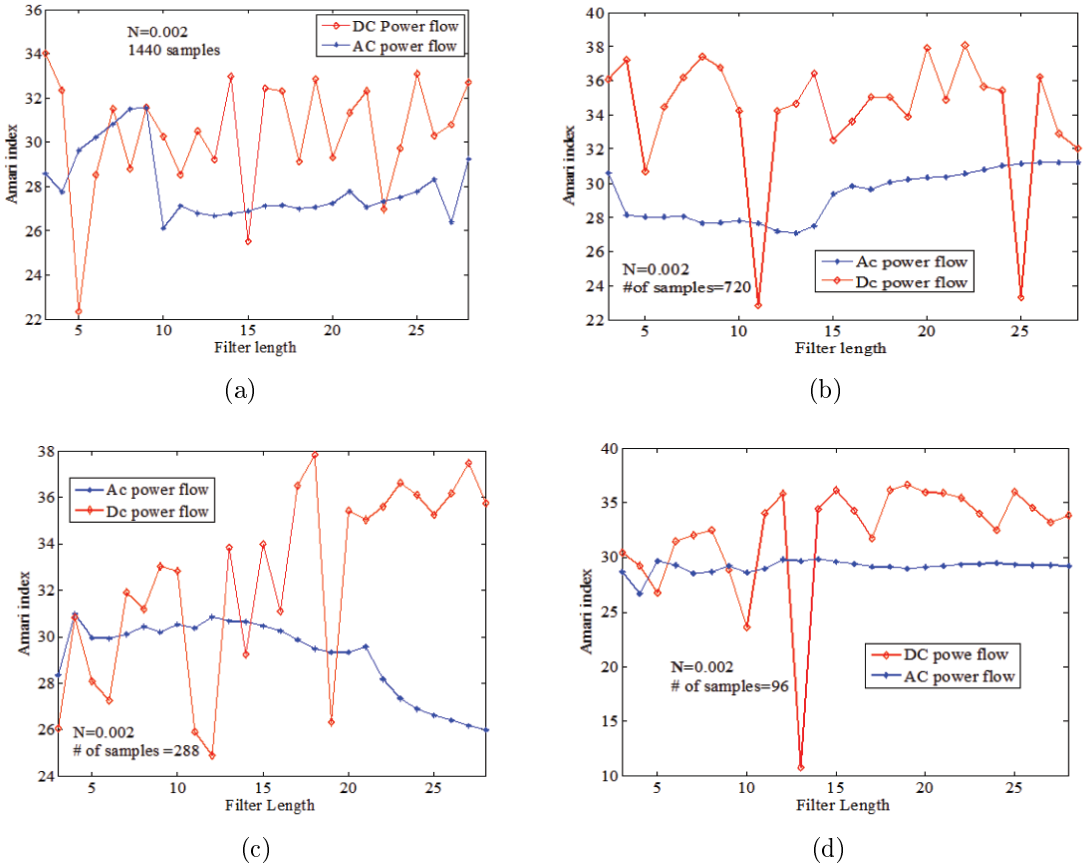

FIGURE 3. Amari index versus filter length for the DC and AC power flow with different samples and 0.002 variance

Figure 4 shows the plot of the 15^{th} IC versus the 5^{th} IC for 720 samples and added Laplace distribution with variance = 0.002. Figures 4(a) and 4(b) are generated for the optimum filter of the ac power flow (MA length = 13) and Figure 4(b) for filter length = 7, whereas Figures 4(c)-4(d) are for the optimum MA length of dc power flow (MA length = 11) and MA length = 7. It is obvious that the optimum filters for both of dc and ac show more independency between the extracted components and less scattering compared to other filter length.

Figure 5 shows the correlation coefficients between the estimated IC components for the model that based on the dc power flow analysis. Figure 5(a) is obtained for filter length of 11 (optimum filter) while Figure 5(b) is for filter length 8. The figure shows that the correlation coefficients for the optimum filter compared to the second filter are lower which imply that the independency between the IC components is higher for the optimum filter. Figure 5 verifies the results obtained in Figure 4.

To investigate the effect of the amount of fluctuation of the fast components, the introduced method is implemented for different values of variance of the added Laplace distribution 0.0002, 0.002, and 0.02. Figures 3(b) and 6(a), 6(b) show the plot for the Amari index versus the filter length with number of samples = 720 and different values of variance. A careful inspection of the figures shows that the models that based on the dc power flow analysis has a clear and a specific optimum filter and also it has more fluctuation compared to the ac models. Moreover, it is clear that the optimum filter length is increased as the variance is increased due to the fact that increasing the noise

required that the filter bandwidth should be decreased, which imply that the filter length is increased.

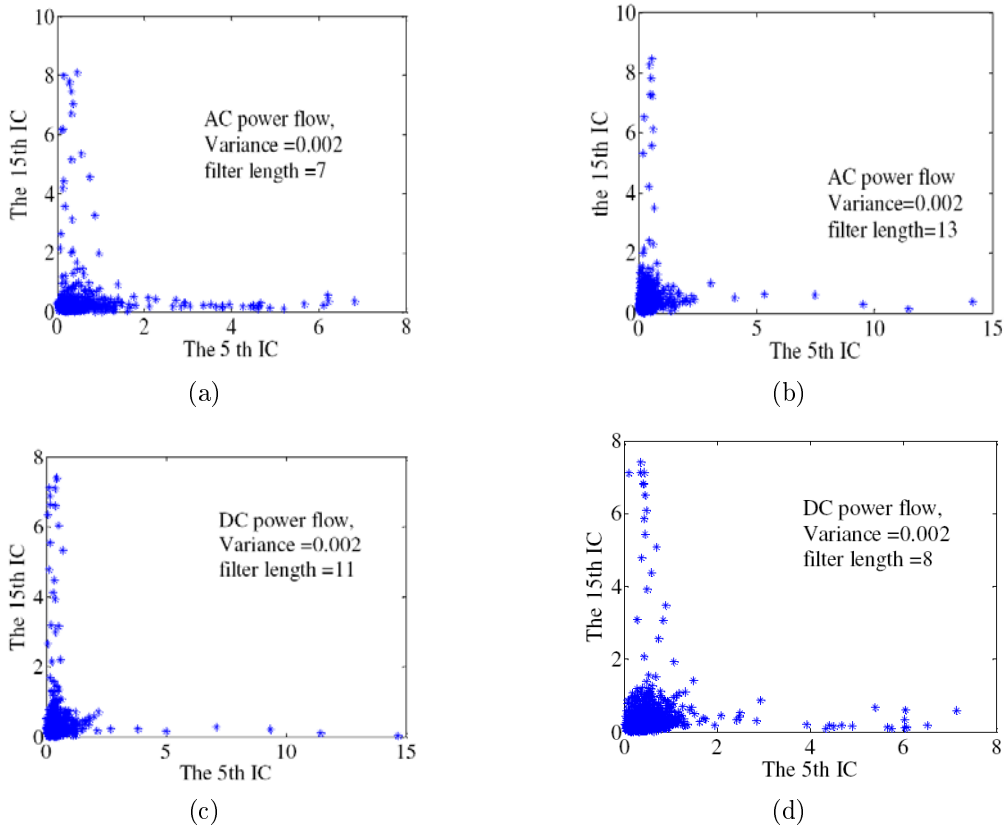

FIGURE 4. The 15^{th} IC versus the 5^{th} IC with 720 samples at variance of 0.002. (a) and (b) for ac power flow at filter length of 7 and the optimum filter length respectively. (c) and (d) for dc power flow for the optimum filter length and 8, respectively.

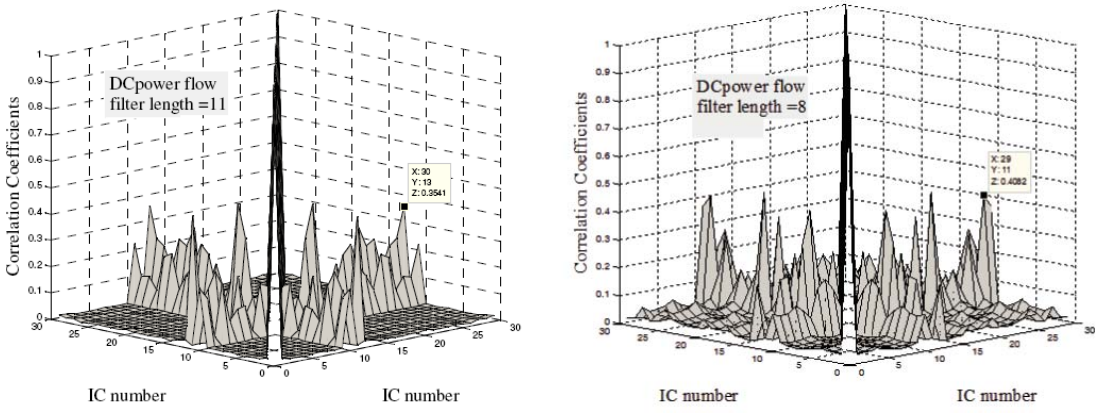

FIGURE 5. The correlation coefficients between the obtained ICs components from using (a) optimum filter for the DC power flow and (b) MA filter with length = 8

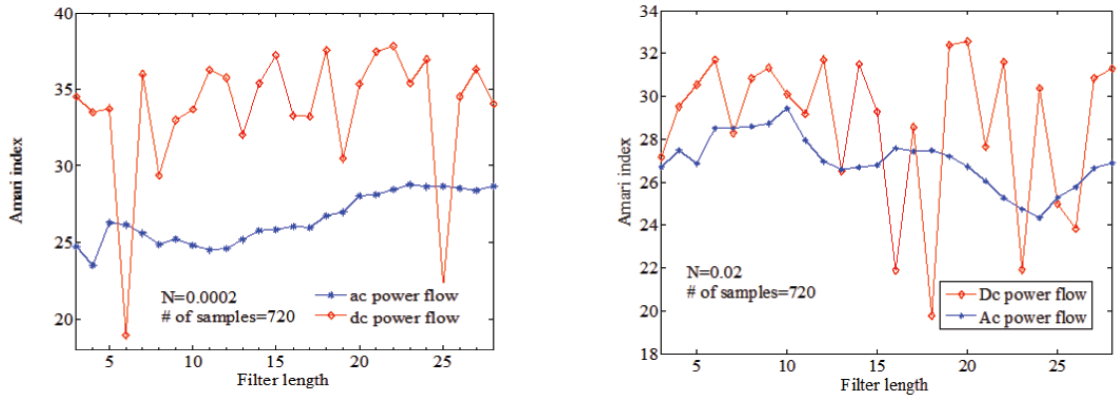

(a) (b)

FIGURE 6. Amari index versus filter length for the DC power flow with 720 samples and (a) 0.0002 and (b) 0.02 variances

6. **Conclusions.** The proposed method is aimed at estimating the appropriate MA filter length. The proposed model combines the ICA and dc or ac power flow analysis to compute the bus voltages, which will be processed using MA filter to separate the fast and slow components. ICA algorithm is applied to fast components to estimate the mixing matrix. Amari index that based on the general global matrix was used to evaluate the ability of the MA filter to separate the independent components (fast fluctuation) and dependent components (slow varying components). This process was repeated for different values of the filter length. From the plot of Amari index versus the filter length, the MA length that produces the minimum index is selected as the optimum filter length.

The proposed method is flexible; it can be used to select the filter length even for the harmonic frequencies, or if there is a variation in the new data relative to the training data. Additionally, using the optimum filter length will lead to a minimum dependency between the fast components, so it can be used in the blind load profile estimation, harmonic analysis, or forecasting problems.

The results show that a high accuracy of estimation is obtained in case of the dc power flow. Regarding the sample size, the results show that the accuracy of estimation of the filter length is increased as the number of samples is increased. A good accuracy to estimate the filter length is achieved even for the smallest size of data used in this work. In our case study, overlearning of the ICA algorithm did not present a problem in our model. The proposed method is quite promising since it is compatible with the measured data each time.

REFERENCES

[1] D. Childers and A. Durling, *Digital Filtering and Signal Processing*, Week St. Paul, MN, 1975.
[2] H. Azami, K. Mohammadi and B. Bozorgtabar, An improved signal segmentation using moving average and Savitzky-Golay filter, *Journal of Signal and Information Processing*, vol.3, pp.39-44, 2012.
[3] S. Smith, *The Scientist and Engineer's Guide to Digital Signal Processing*, California Technical Publishing, 1999.
[4] S. Kundu, *Analog and Digital Communications*, Pearson Education India, 2010.
[5] C. A. Glasby and G. W. Horgan, *Image Analysis for the Biological Sciences*, Wiley, New York, 1995.
[6] W. Rebizant, J. Szafran and A. Wiszniewski, *Digital Signal Processing in Power System Protection and Control*, Springer, 2011.

[7] Y. Zhu, H. Mao, P. Li and Y. Wu, Measurement of lettuce leaf chlorophyll content by means of VIS-NIR spectroscopy, *International Conference on Remote Sensing, Environment and Transportation Engineering*, China, 2011.
[8] J. L. Guiñón, E. Ortega, J. García-Antón and V. Pérez-Herranz, Moving average and Savitzki-Golay smoothing filters using Mathcad, *International Conference on Engineering Education*, Coimbra, Portugal, 2007.
[9] S. Dash, A comparative study of moving averages filter: Simple, weighted and exponential, *Trade Station Labs, Analysis Concepts*, no.38, 2012.
[10] M. Yanagi, M. Sone and R. Horie, Toward a brain-computer interface based on perception of audio-visual temporal asynchrony: A near-infrared spectroscopy study, *Transactions of Japanese Society for Medical and Biological Engineering*, vol.51, 2013.
[11] A. Chaddad, Brain function diagnosis enhanced using Denoised fNIRS raw signals, *Journal of Biomedical Science and Engineering*, vol.7, pp.218-227, 2014.
[12] A. Nakata, A. Ueda and A. Torii, A method of current detection for an active power filter applying moving average to pq-theory, *Power Electronics Specialists Conference*, 1998.
[13] A. Ohyagi, A. Ueda, A. Torii and H. Takai, Ultra-fast response control system for active power filter, *Power Conversion Conference*, Osaka, vol.2, 2002.
[14] F. D. Freijedo et al., Novel harmonic identification algorithm based on Fourier correlation and moving average filtering, *Power Conversion Conference*, vol.2, Osaka, 2002.
[15] F. D. Freijedo, J. Doval-Gandoy, O. Lopez and J. Cabaleiro, Harmonic identification methods based on moving average filters for active power filters, *IEEE Industry Applications Society Annual Meeting*, 2008.
[16] J. Luukko and K. Rauma, Open-loop adaptive filter for power electronics applications, *IEEE Trans. Industrial Electronics*, vol.55, no.2, 2008.
[17] K. Nose-Filho, A. D. P. Lotufo and C. R. Minussi, Preprocessing data for short-term load forecasting with a general regression neural network and a moving average filter, *IEEE Trondheim in PowerTech*, 2011.
[18] J. Forbes, M. Ordonez and M. Anun, Improving the dynamic response of power factor correctors using simple digital filters: Moving average filter comparative evaluation, *IEEE Energy Conversion Congress and Exposition*, 2013.
[19] B. L. Eidson, D. L. Geiger and M. Halpin, Equivalent power system impedance estimation using voltage and current measurements, *IEEE Conference on Power Systems*, Clemson University, 2014.
[20] H. W. Liao and D. Niebur, Load profile estimation in electric transmission networks using independent component analysis, *IEEE Trans. Power Systems*, vol.18, pp.707-715, 2003.
[21] D. Niebur, E. Gursoy and H. Liao, Independent component analysis techniques for power system load estimation – A signal-processing approach, *Applied Mathematics for Restructured Electric Power – Optimization, Control, and Computational Intelligence*, New York, USA, Springer, 2004.
[22] E. Gursoy and D. Niebur, On-line estimation of electric power system active loads, *International Joint Conference on Neural Networks*, Vancouver, BC, Canada, pp.1689-1694, 2006.
[23] H. Liao and D. Niebur, Estimating reactive load profiles using independent component analysis, *International Conference on Intelligent System Applications to Power Systems*, Lemnos, Greece, 2003.
[24] P. Supriya and T. N. P. Nambiar, Blind signal separation of harmonic voltages in non-linear loads, *J. Electrical Systems*, vol.8, no.4, pp.433-441, 2012.
[25] H. Liao and D. Niebur, Exploring independent component analysis for electric load profiling, *Proc. of International Joint Conference on Neural Networks*, vol.3, 2002.
[26] D. Niebur, A. Rotolo and F. Mazzoleni, Load profile separation using independent component analysis, *International Conference on Intelligent System Applications to Power Systems*, Budapest, Hungary, 2001.
[27] E. Gursoy and D. Niebur, Harmonic load identification using complex independent component analysis, *IEEE Trans. on Power Delivery*, vol.24, no.1, pp.285-292, 2009.
[28] P. Supriya and T. N. P. Nambiar, Harmonic current estimation using blind signal processing techniques, *Proc. of IEEE Conference on Signal Processing, Communication, Computing and Network Technologies*, Kanyakumari, India, pp.107-111, 2011.
[29] P. Supriya and T. N. P. Nambiar, Estimation of harmonic voltages using independent component analysis, *Proc. of IET Conference on Sustainable Energy and Intelligent Systems*, Chennai, India, 2011.

[30] E. Gursoy and D. Niebur, Blind source separation techniques for harmonic current source estimation, *Power Systems Conference and Exposition*, pp.252-255, 2006.
[31] K. Siwek, S. Osowski, R. Szupiluk, P. Wojewnik and T. Ząbkowski, Blind source separation for improved load forecasting in the power system, *Proc. of the 2005 European Conference on Circuit Theory and Design*, vol.3, pp.61-64, 2005.
[32] A. Cichocki and S. Amari, *Adaptive Blind Signal and Image Processing*, John Wiley & Sons, Chichester, 2006.
[33] A. Cichocki, S. I. Amari and H. Yang, A new learning algorithm for blind source separation, *Proc. of Advances in Neural Information Processing*, pp.757-763, 1996.
[34] E. Hirst and B. Kirby, Defining intra- and interhour load swings, *IEEE Trans. Power Systems*, vol.13, pp.1379-1385, 1998.
[35] I. T. J. Berlin, *Principal Component Analysis*, Springer-Verlag, 1986.
[36] A. Al-odienat and T. Gulrez, Inverse covariance principal component analysis for power system stability studies, *Turk J. Elec. Eng. & Comp. Sci.*, vol.22, pp.57-65, 2014.
[37] E. Oja, A. Hyvarinen and J. Karhunen, *Independent Component Analysis: Adaptive and Learning Systems for Signal Processing Communication and Control Series*, John Wiley & Sons Inc., 2002.
[38] A. Hyvärinen, Independent component analysis for time-dependent stochastic processes, *Proc. of International Conference on Artificial Neural Networks*, Skovde, Sweden, pp.541-546, 1998.
[39] K. Zhang and L.-W. Chan, An adaptive method for subband decomposition ICA, *Neural Computation Jan.*, vol.18, no.1, pp.191-223, 2006.
[40] H.-M. Park, S.-H. Oh and S.-Y. Lee, A filter bank approach to independent component analysis and its application to adaptive noise cancelling, *Neurocomputing*, vol.55, p.611, no.3-4, pp.755-759, 2003.
[41] J. Chen and X. Z. Wang, A new approach to near-infrared spectral data analysis using independent component analysis, *J. Chem. Inf. Comput. Sci.*, vol.41, pp.992-1001, 2001.
[42] Y.-K. Chuang, S. Chen, Y. M. Lo, C.-Y. Tsai, I.-C. Yang, Y.-L. Chen, P.-J. Pan and C.-C. Chen, Integration of independent component analysis with near infrared spectroscopy for rapid quantification of sugar content in wax Jambu (Syzygiumsamarangense Merrill & Perry), *Journal of Food and Drug Analysis*, vol.20, no.4, pp.855-864, 2012.
[43] J. V. Stone, *Independent Component Analysis: A Tutorial Introduction*, Massachusetts Institute of Technology, 2004.
[44] H. Aapo, *Survey on Independent Component Analysis*, http://www.stat.rutgers.edu/home/rebecka/Stat687/NCS99.pdf.
[45] J. F. Cardoso, High-order contrasts for independent component analysis, *Neural Computation*, vol.583, no.11, pp.157-192, 1999.
[46] C. G. Puntonet and A. Prieto, Independent component analysis and blind signal separation, *The 5th International Conference*, Granda, Spain, 2004.
[47] J. M. Mendal, Tutorial on higher order statistics (spectra) in signal processing and system theory: Theoretical results and some applications, *Proc. of the IEEE*, vol.79, no.3, pp.278-305, 1991.
[48] S. Kundu, *Analog and Digital Communications*, Pearson Education India, 2010.
[49] G. C. Chen, P. Wang and J. Yu, Application of independent component analysis in short-term power forecasting of wind farm, *Applied Mechanics and Materials*, vol.63-64, pp.124-128, 2011.
[50] A. Hyvärinen, Fast and robust fixed-point algorithms for independent component analysis, *IEEE Trans. Neural Networks*, vol.10, no.3, pp.626-634, 1999.
[51] E. B. A. Hyvarinen, A fast fixed-point algorithm for independent component analysis of complex valued signals, *Int. J. of Neural Systems*, vol.10, pp.1-8, 2000.
[52] A. Bell and T. Sejnowski, An information maximization approach to blind separation and blind deconvolution, *Neural Computation*, vol.7, no.6, pp.1129-1159, 1995.
[53] P. A. D. F. R. Højen-Sørensen, O. Winther and L. K. Hansen, Mean-field approaches to independent component analysis, *Neural Computation*, vol.14, no.4, pp.889-918, 2002.
[54] F. R. Bach and M. I. Jordan, Kernel independent component analysis, *Journal of Machine Learning Research*, vol.3, pp.1-48, 2002.
[55] G. Arfken and G.-S. Orthogonalization, *Mathematical Methods for Physicists*, 3rd Edition, Academic Press, Orlando, FL, 1985.
[56] J. Nearing, *Mathematical Tools for Physics*, University of Miami, 2003.
[57] C. Moler, *Numerical Computing with MATLAB*, MathWorks, 2004.
[58] T. Tanaka and A. Cichocki, Subband decomposition independent component analysis and new performance criteria, *IEEE International Conference on Acoustics, Speech, and Signal Processing*, 2004.
[59] *http://www.nirpublications.co.uk/discus/messages/5/318.html?/094479005.*

[60] The Electric Reliability Council of Texas, *Load Profiling*, http://www.ercot.com/Participants/load profiling.htm.
[61] S. Kotz, T. J. Kozubowski and K. Podgórski, *The Laplace Distribution and Generations*, Birkhäuser, 2001.
[62] S. Inusah and T. Kozubowski, A discrete analogue of the Laplace distribution, *Journal of Statistical Planning and Inference*, vol.136, pp.1090-1102, 2006.
[63] R. D. Zimmerman, C. E. Murillo-Sánchez and D. Gan, *A MATLAB Power System Simulation Package*, http://www.pserc.cornell.edu//matpower/.
[64] *Package 'JADE'*, http://perso.telecom/paristech.fr/∼cardoso/guidesepsou.html.
[65] *http://cran.r-project.org/web/packages/JADE/JADE.pdf.*
[66] M. Joho, H. Mathis and R. H. Lambert, Over determined blind source separation: Using more sensors than source signals in a noisy mixture, *ICA*, Helsinki, Finland, pp.81-89, 2000.
[67] E. Gursoy and D. Niebur, Impact of sample size on ICA-based harmonic source estimation, *The 13th International Conference on Intelligent Systems Application to Power Systems*, pp.123-127, 2005.